Simulation of Semiconductor Processes and Devices 2016
Edited by E. Bär, J. Lorenz, and P. Pichler

NEMO5: Predicting MoS_2 Heterojunctions

Kuang-Chung Wang*, Daniel Valencia, James Charles, Yu He, Michael Povolotskyi, Gerhard Klimeck,
Jesse Maassen, Mark Lundstrom, Tillmann Kubis
School of Electrical and
Computer Engineering
Purdue University
Email: wang2366@purdue.edu

***Abstract*—Molybdenum disulfide (MoS_2) is a promising 2D material since it has a finite band gap, and its electronic band structure depends on the layer thickness. The tunability of the gate voltage on band alignment of different MoS_2 layers is analyzed. For this purpose, the multipurpose nanodevice simulation tool NEMO5 was altered by several new features: electronic bandstructure calculations in maximally localized Wannier function (MLWF) representation and self-consistent charge calculations with subatomic electrostatic resolution.**

I. Introduction

MoS_2 is a promising material candidate for next generation nano-devices due to few-atom device thickness and best imaginable gate control. In contrast to e.g. graphene, MoS_2 offers a finite band gap which makes it suitable for transistors [1] to have a smaller off-current.

It is also shown to have a wide range of material characteristics depending on the layer thickness. The band-gap decrease from 1.8 eV to 0.9 eV [2] from bulk to mono-layer(ML) and is indirect for two-layer and the thicker films while direct for a single layer MoS_2. A geometry induced heterojunction [3] can therefore be formed with a discontinuity of layer thickness. The wide range of band structure characteristics provided are interesting for thin and flexible optoelectronics e.g. photodetectors[4] [5], LED [6]. To contribute to both applications, the band offset variation with different layer thicknesses and its gate field dependence is assessed here. With the calculation of electron affinity, the junction type can be determined and predict the transport across the junction.

To represent the hamiltonian of the system, empirical tight binding model(ETB) [7] and density functional theory(DFT) [8] are available. The intensive computation requirement for DFT and non-transferability of van der Waals induced interlayer coupling with ETB have lowered the application to device simulation and prediction. In this paper, Wannier functions are used and transferability is shown for different layer of Van der Waals layered structures.

A. Methodology

MoS_2 with trigonal prismatic polytype, known as "2H" symmetry, in the bulk form is used. The electronic Hamiltonian and basis functions of density functional theory simulations (GGA with PBE [9]) are calculated with the VASP software [10]. The structure is relaxed with a convergence criterion of 10^{-8}eV in between iterations of a self-consistent electronic calculation.

With the Wannier90 software[11], the electronic Hamiltonian of a MoS_2 unit cell in MLWF representation is transformed from the original basis. The initial projection basis includes d orbitals with Molybdenum and p orbitals for Sulfur atoms. The spreading of the Wannier function, defined in Eq. 1, is reduced iteratively and 2 $\AA^2$ achieved in the end.

$$\Omega = [\langle r^2 \rangle - \bar{r}^2] \tag{1}$$

This unit cell Hamiltonian is repeated in the NEMO5 software [12] to generate a real-size device Hamiltonian and solve for electronic densities. For charge self-consistency, the Schrödinger equation is iteratively solved with the Poisson equation in sub-atomic resolution, simplifying the spatial shape of Wannier functions with Gaussian functions with a standard deviation of 0.14 nm(square root of the Ω in Eq. 1). All assessed structures are close to the experimental setups of Ref. [3] with a consistently scaled oxide and gate voltage.

A metal oxide semiconductor structure is set up as shown in Fig. 1. The equivalent oxide thickness is set to be 12.36 nm. The channel consists of one to ten layers of MoS_2 with donor doping $1.5 \times 10^{18}\,\mathrm{cm}^{-3}$. On the gate side, a Dirichlet boundary condition is used to set the gate voltage value. The top side is exposed to vacuum and a Neumann boundary condition of flat band (zero electric field) is applied. Bandstructure is calculated and the response to different gate voltages, doping and layer thickness are analyzed.

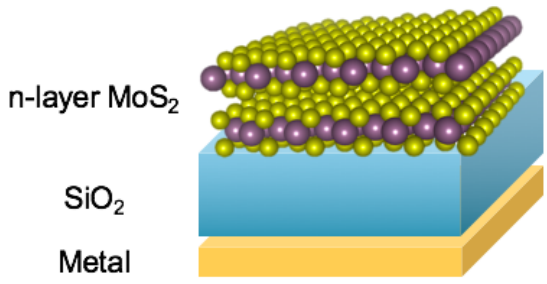

Fig. 1. Schematics of the metal-oxide semiconductor structure simulated in this paper. Gate is on the bottom and vacuum on the top with varying thickness of MoS_2 layer.

978-1-5090-0818-6/16/$31.00

B. Discussion

After a structure relaxation, a lattice constant with a = 3.18 Å and c = 12.48 Å are used [13]. The MLWF-calculated bandstructures are found to agree very well with ab-initio calculations, Fig.2 and Fig.3, for any MoS_2 layer thickness with an interaction radius of 1.2 nm. The conduction band minimum in 2D momentum space is shown in Fig.4. Two inequivalent valleys exist with non-isotropic and layer dependent effective masses (in agreement with Ref.[14]). The K valley has an average DOS effective mass of 0.62 m_0 increasing with the layer thickness, while the Λ valley is about $0.52m_0$ decreasing with the number of layers.

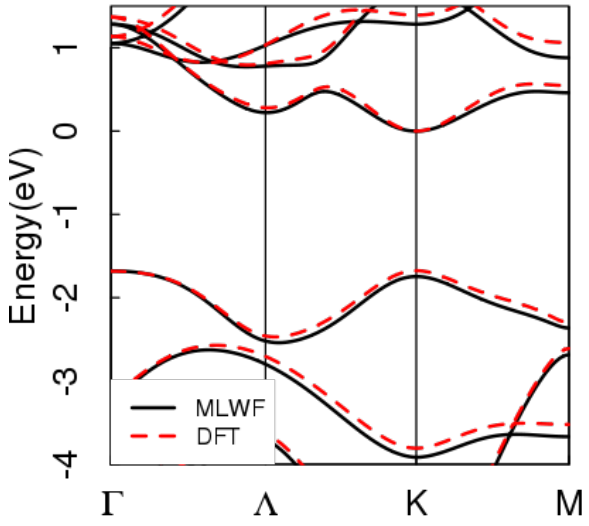

Fig. 2. Comparison of mono-layer MoS_2 band diagrams solved with MLWF in NEMO5 and the DFT functionality of VASP. The agreement confirms the transferability of the MLWF parameters.

The conduction band edge relative to the Fermi level as a function of numbers of layers and gate bias is given in Fig.5. Both the layer thickness and the applied bias show a significant impact on the conduction band edge. The energy difference of the K and Λ valleys is shown in Fig. 6. The crossover of the conduction band minimum from K to Λ valley illustrated in this figure is the reason for the minimum of conduction band edge in Fig.5 .

Figure 7 compares the band structure of a 5-layer thick MoS_2 system with and without a finite gate bias applied. Without electric fields, the K-valley is 5-fold degenerate. The finite gate field lifts this degeneracy and reduces the energy separation between K and Λ valleys. The wave function is spatially resolved for the three lowest eigenstates at these two valleys in Fig. 8 and Fig.9. The Λ valley states are shown to have a strong interlayer coupling and extend across the layers. In contrast, K valley wavefunctions are very localized.

II. Conclusion

The nanodevice simulation tool NEMO5 was altered to accurately describe MoS_2 electrons in MLWF representation.

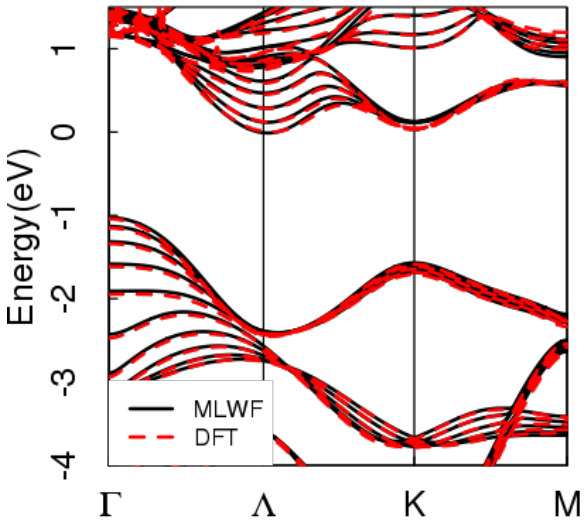

Fig. 3. Comparison of five-layer MoS_2 band diagrams solved with MLWF in NEMO5 and the DFT functionality of VASP. The agreement confirms the transferability of the MLWF parameters.

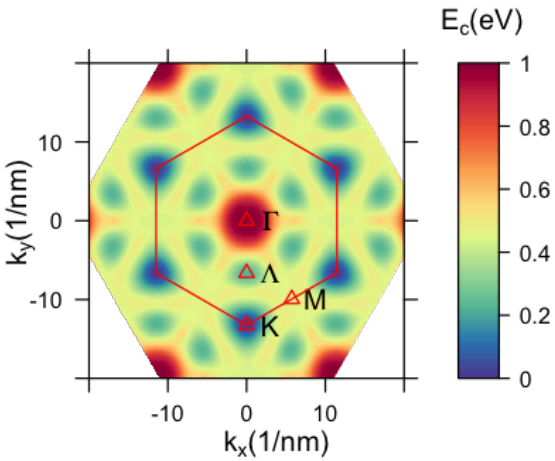

Fig. 4. Contour graph of the minimum of the conduction band for mono-layer MoS_2. The red hexagon depicts the first Brillouin zone.

All MLWF Hamiltonians are verified against ab-initio models. Hetero-junctions of different layers show band misalignment as a function of gate voltages. Distinct valleys are tunable with layer thickness and applied gate voltage.

Acknowledgment

The work is supported by NSF EFRI-1433510. We also acknowledge the Rosen Center for Advanced Computing at Purdue University for the use of their computing resources and technical support. This research is part of the Blue Waters sustained-petascale computing project, which is supported by the National Science Foundation (award number ACI 1238993) and the state of Illinois. Blue Waters is a joint effort of the University of Illinois at Urbana-Champaign and

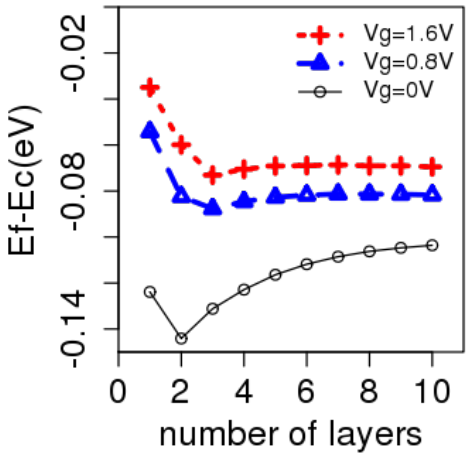

Fig. 5. Conduction band minima of MoS_2 structures with different layer thicknesses as shown in Fig. 1 and different gate bias voltages.

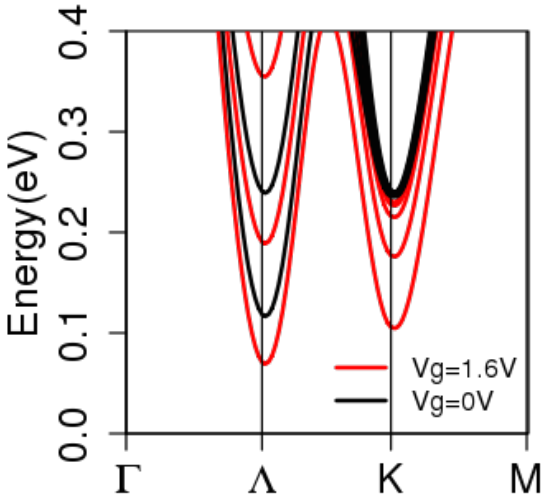

Fig. 7. Bandstructures of a 5-layer MoS_2 system as shown in Fig. 1 with and without finite gate voltage. The gate field lifts the degeneracy at the K valley while it only shifts Λ valley energies.

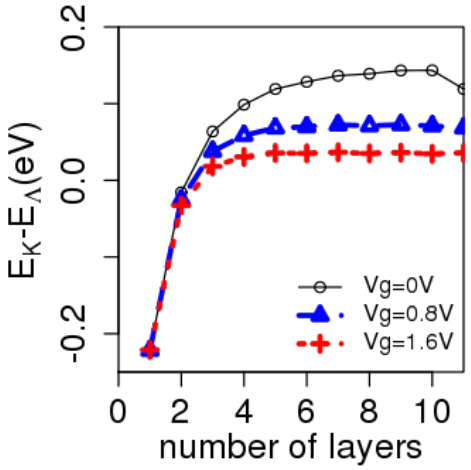

Fig. 6. Energy difference between the K and Λ valleys of a MoS_2 structure with different number of layers as shown in Fig. 1 and for different gate bias voltages.

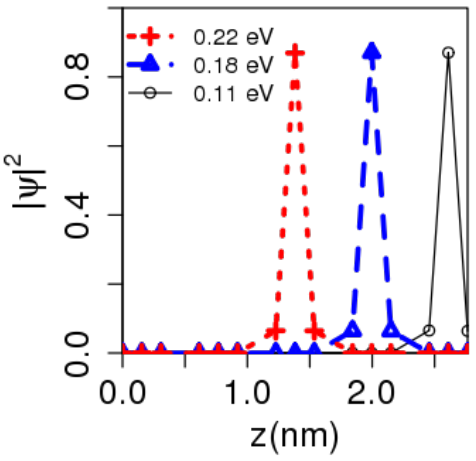

Fig. 8. Absolute squared wave function of the three lowest K valley eigenstates of the 5 layer MoS2 device of Fig. 7 at Vg =1.6V.

its National Center for Supercomputing Applications. This work is also part of the Accelerating Nano-scale Transistor Innovation with NEMO5 on Blue Waters PRAC allocation support by the National Science Foundation (award number OCI-0832623).

References

[1] B. Radisavljevic, A. Radenovic, J. Brivio, V. Giacometti, and A. Kis, "Single-layer MoS2 transistors," *Nat. Nanotechnol.*, vol. 6, no. 3, pp. 147–50, 2011.

[2] W. S. Yun, S. Han, S. C. Hong, I. G. Kim, and J. Lee, "Thickness and strain effects on electronic structures of transition metal dichalcogenides: 2H-MX2 semiconductors (M = Mo, W; X = S, Se, Te)," *Phys. Rev. B*, vol. 85, no. 3, pp. 1–5, 2012.

[3] S. L. Howell, D. Jariwala, C.-C. Wu, K.-S. Chen, V. K. Sangwan, J. Kang, T. J. Marks, M. C. Hersam, and L. J. Lauhon, "Investigation of Band-Offsets at MonolayerMultilayer MoS 2 Junctions by Scanning Photocurrent Microscopy," *Nano Lett.*, vol. 15, p. 2278, 2015.

[4] M. R. Esmaeili-Rad and S. Salahuddin, "High Performance Molybdenum Disulfide Amorphous Silicon Heterojunction Photodetector," *Sci. Rep.*, vol. 3, p. 2345, 2013.

[5] M. S. Choi, D. Qu, D. Lee, X. Liu, K. Watanabe, T. Taniguchi, and W. J. Yoo, "Lateral MoS2 p-n junction formed by chemical doping for use in high-performance optoelectronics," *ACS Nano*, vol. 8, no. 9, pp. 9332–9340, 2014.

[6] F. Withers, O. Del Pozo-Zamudio, A. Mishchenko, a. P. Rooney, A. Gholinia, K. Watanabe, T. Taniguchi, S. J. Haigh, a. K. Geim, a. I. Tartakovskii, and K. S. Novoselov, "Light-emitting diodes by band-

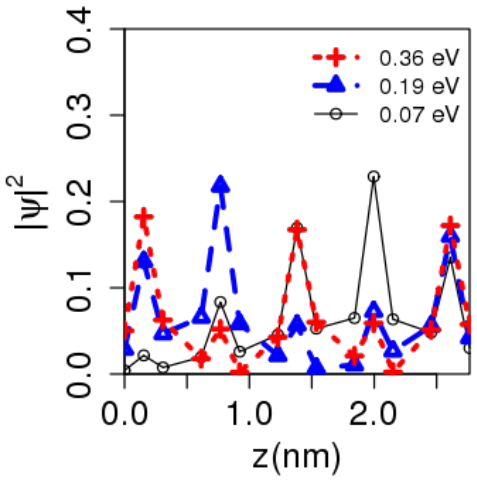

Fig. 9. Absolute squared wave function of the three lowest Λ valley eigenstates of the 5 layer MoS2 device of Fig. 7 at Vg =1.6V.

structure engineering in van der Waals heterostructures," *Nat. Mater.*, vol. 14, no. February, pp. 301–306, 2015.

[7] G. Klimeck, S. S. Ahmed, N. Kharche, M. Korkusinski, M. Usman, M. Prada, and T. B. Boykin, "Atomistic simulation of realistically sized nanodevices using NEMO 3-D-Part II: Applications," *IEEE Trans. Electron Devices*, vol. 54, no. 9, pp. 2090–2099, 2007.

[8] J. Maassen, M. Harb, V. Michaud-Rioux, Y. Zhu, and H. Guo, "Quantum transport modeling from first principles," *Proc. IEEE*, vol. 101, no. 2, pp. 518–530, 2013.

[9] J. Perdew, K. Burke, and Y. Wang, "Generalized gradient approximation for the exchange-correlation hole of a many-electron system," *Phys. Rev. B*, vol. 54, no. 23, pp. 16 533–16 539, 1996.

[10] G. Kresse and J. Furthmüller, "Efficient iterative schemes for ab initio total-energy calculations using a plane-wave basis set," *Phys. Rev. B*, vol. 54, no. 16, pp. 11 169–11 186, 1996.

[11] N. Marzari and D. Vanderbilt, "Maximally-localized generalized Wannier functions for composite energy bands," *Phys. Rev. B*, vol. 56, no. 20, p. 12847, 1997.

[12] S. Steiger, M. Povolotskyi, H. H. Park, T. Kubis, and G. Klimeck, "NEMO5: A parallel multiscale nanoelectronics modeling tool," *IEEE Trans. Nanotechnol.*, vol. 10, no. 6, pp. 1464–1474, 2011.

[13] F. Jellinek, G. Brauer, and H. Müller, "Molybdenum and Niobium Sulphides," *Nature*, vol. 185, no. 4710, pp. 376–377, feb 1960.

[14] H. Heo, J. H. Sung, S. Cha, B.-G. Jang, J.-Y. Kim, G. Jin, D. Lee, J.-H. Ahn, M.-J. Lee, J. H. Shim, H. Choi, and M.-H. Jo, "Interlayer orientation-dependent light absorption and emission in monolayer semiconductor stacks (Supporting Information)," *Nat. Commun.*, vol. 6, no. 2, p. 7372, 2015.